APPLICATION OF THE 3D-EHLA PROCESS FOR AGILE ALLOY DEVELOPMENT

Marie-Noemi Bold[1], Nico Schmitt[1], Prof. Johannes Henrich Schleifenbaum[1]
[1]Chair Digital Additive Production – RWTH Aachen University, Germany

ABSTRACT

The development of new high-performance alloys is a key factor for innovation and technological advances. However, the conventional development route by means of casting is not designed to facilitate a high-throughput alloy development, since in general only one alloy composition can be made per cast and process inherent challenges like macrosegregations occur when dealing with highly alloyed materials. The newly developed 3D Extreme High Speed Laser Material Deposition (EHLA) process shows promising features for an accelerated alloy development for metal powder-based AM processes. In this work, the applicability of the 3D-EHLA process in the context of rapid alloy development is investigated. In the first step, the parameters (e.g. process speed, laser power, powder mass flow) and tools (powder-gas jet, laser radiation) of the 3D-EHLA process and their effect on alloy development processes are evaluated. Subsequently, an integrated methodology is proposed, through which an efficient workflow along the whole process chain of alloy manufacturing and sample evaluation is obtainable. Finally, the influence of laser power, process speed and powder mass flow on the evolution of the microstructure is investigated (alloy: 316L). The most pronounced influence of these parameters is found for the process speed, which displays a negative correlation to the cell size. A positive correlation is found between laser power/powder mass flow and the cell size.

Keywords: Additive Manufacturing, Extreme High-Speed Laser Material Deposition, 3D-EHLA, Rapid Alloy Development, High-Entropy Alloys, Laser Metal Deposition

INTRODUCTION

To ensure ongoing technological advances and the accompanying spread of prosperity [1], there is a constant need for new materials [2]. The development route by traditional production processes is thereby often characterized by a lengthy and cost-intensive Trial-and-Error approach [3,4]. Additive Manufacturing (AM) offers new kinds of design freedom regarding the material mixing in the powder-based form [5], which can enable a significant acceleration of the alloy development [6]. Furthermore, special process conditions like high cooling rates of more than 10^7 K/s [7] in comparison to casting (10-10^2 K/s) [8] open up the potential for AM to enable the manufacturing of new high-performance materials. Since a fast development of customized alloys is desirable, efficient and effective methodologies for alloy development need to be outlined and validated. A promising tool for a potential methodology is the 3D-EHLA process, in which alloys and elemental powders can be mixed in situ by a nozzle-based powder supply and processed immediately, while the microstructure can be altered by changing the cooling rate in the range of 10^2-10^7 K/s [9]. In comparison to the batch-wise testing used in casting, this agile alloy development enables a drastic reduction of the development time, since numerous samples in various chemical compositions can be manufactured in short periods of time [10].

Despite advances in the understanding of the chemical and physical processes involved in alloy formation, it currently takes decades to bring a new alloy from the research stage to commercial application [11]. Conventionally, the alloy to be examined is melted in a laboratory scale and cast

subsequently. This results in limitations with regard to the alloy composition, for example in the case of material combinations with poor castability or due to process-inherent challenges such as macrosegregations [12,13]. The casting can then be formed and heat treated further in order to change the microstructure and thus the properties of the material [4]. Since the analysis becomes increasingly complex when examining multiple compositions, forming and heat treatment steps, traditional alloy development often focuses on a basic element, whose properties are altered by a small addition of alloying elements in the single-digit percentage range [14]. As a result, phase diagrams are mainly explored at the edges, while a large portion of the possible phase space remains untouched [15].

However, promising material classes such as High-entropy alloys (HEAs) consist of five or more elements in near-equimolar or equimolar composition [16]. Since this class of materials is located in relatively unexplored areas of the corresponding phase diagrams and contains a large number of possible alloy compositions, there is an increased need for the rapid screening of complex alloy compositions [15]. In addition to the currently dominant field of application for AM, prototype construction [17], the increased design freedom compared to conventional processes can also be used for agile alloy development by utilizing the simplicity of dynamic material alterations via powder blends or in situ powder mixing [3,18,19]. Due to the growing market for metal AM, there is an interest in developing materials and alloys tailored to the opportunities of these manufacturing processes, possibly even directly by AM.

Two common AM processes are Laser Powder Bed Fusion (LPBF) and Laser Metal Deposition (LMD). While only prefabricated powder blends can be used within a LPBF process [19], LMD offers the potential to produce several different alloys in a single process step by using multiple powder hoppers simultaneously. Such an applicability of the LMD process for alloy development was shown by STEEN et al. in 1993 for three powder hoppers filled with elemental powders: the powder feed rates of each powder hopper were adjusted during the process to deposit material with alloy gradients [20]. The Extreme High Speed Laser Material Deposition (EHLA) process, developed based on conventional LMD, was introduced in 2015 and features significantly higher process speeds of up to 500 m/min [21] (LMD: typically 0,5-2 m/min [22–24]).

1. PROCESS AND ENGINEERING RELATED CHALLENGES OF EHLA

In the EHLA process, the focus of the powder-gas jet is shifted perpendicularly to the components surface compared to the LMD process setting. The powder material is therefore melted above the components surface, which enables process speeds up to 500 m/min [22], see Fig. 1.

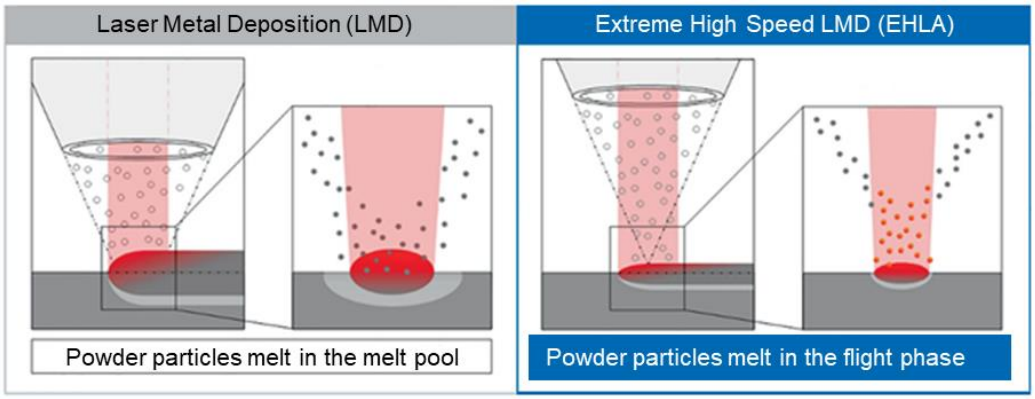

Fig. 1: Schematic comparison of LMD and EHLA (modified from [25, p.40])

Due to the greater process speed, the melt pool is smaller using EHLA, which results in less dilution (< 1% [26]). This leads to a layer composition which is closer to the desired composition and less influenced by the dilution with the base material (see Fig. 1). In addition, the heating and cooling rates for EHLA are greater than for LMD due to the shorter laser-material interaction times. With EHLA, thin layers with a minimum thickness of up to 25 µm can be produced and a powder mass flow of 50 g/min and higher can be achieved [27], while a powder mass flow of 5-15 g/min is commonly used with LMD [28,29].

Despite the improvements of EHLA compared to the conventional LMD process, such as a high powder efficiency of up to 95% even at high lateral resolution [22] and a reduced roughness of the deposited layers [30], EHLA is primarily used for the coating of rotationally symmetrical components and not applied to three-dimensional free-form structures [31]. This is due to the necessary accelerations and velocities, which are easier to obtain by rotation of the specimen itself. Furthermore, EHLA is not suitable for hybrid-additive repair or the AM of complex structures [27]. A process that paves the way to the third dimension based on EHLA could have the potential to revolutionize the AM of metallic materials.

2. PROCESS CHARACTERISTICS OF 3D-EHLA

Based on the successful development of EHLA as an efficient and environmentally friendly coating process [21], the 3D-EHLA process is being developed. It aims to expand the field of application of the new EHLA technology from simple, rotationally symmetrical components to individual, complex geometries. The focus no longer lies on pure coating, but particularly on additive manufacturing as well as agile alloy development. The term agile alloy development is used to emphasize an improvement compared to the established term Rapid Alloy Development (RAD) with regard to adjustability of cooling rates (compared to LMD [32]) and flexibility of composition changes (compared to LPBF [19]). Nonetheless, the term RAD is used in the rest of this work to establish a consistent terminology within the literature. For use in additive manufacturing, the 3D-EHLA process, which is currently exclusively available on the pE3D system by ponticon GmbH, achieves the necessary process speeds in a small space using three linear motors in a tripod structure [9]. This enables a targeted control in three cartesian coordinates, and thus the production of different sample geometries for the RAD. The pE3D system is capable of process speeds of up to 200 m/min, an acceleration of up to 5g (approx. 50 m/s^2), a maximum payload 25 kg and a maximum build volume of 0,5 x 0,5 x 0,5 m^3 [27]. For great material mixing freedom, up to eight powder hoppers can be connected to the pE3D system and be used simultaneously. The melting behavior of both substrate and powder and thus the alloy formation during the process can be influenced by a variably adjustable laser power. Due to the long powder conveying distance, there is a start-up and run-down time in which no constant powder mass flow is present at the powder nozzle. Therefore, the powder feed usually remains active between process steps. The resulting overspray leads to increased powder consumption and contamination of the powder. By using rapid powder-switches, which are installed near the powder nozzle, switching cycles of less than 200 ms can be achieved. The powder is collected in containers during start-up and run-down times as well as between process steps and can be reused, which increases powder efficiency and saves both resources and costs. [33]

3. SUITABILITY OF THE 3D-EHLA PROCESS FOR RAPID ALLOY DEVELOPMENT

3.1 REQUIREMENTS AND TECHNIQUES OF RAD

Combinatorial methods, which are characterized in materials science by the synthesis of many samples with different parameters (composition, cooling rate, etc.) in a short time, have potential for use in RAD [18]. The entirety of samples manufactured in this way is referred to as an "alloy library". This approach enables both the improvement of existing alloy systems and the investigation of new ones. To be able to implement it, suitable methods are required both for the rapid production of many different samples (several dozen per day) and subsequent characterization. This work focuses on the former.

Since the parameter selection for combinatorial methods can no longer be based on the experience of a metallurgist due to the sheer volume of data points, the support of computer-based algorithms in the context of digitalization is becoming increasingly important [34]. BOYCE et al. see the future of material development in that engineers define the requirements for an alloy and an artificial intelligence (AI) calculates the optimal composition and process route based on a database [35]. However, the use of AI for material development is currently mostly unexplored [36] and experimental validation will always be necessary [13]. In the area of metallic materials, the RAD was typically carried out using methods such as PVD in the past, whereby only very thin layers (1-5 µm) of the alloys are formed [37–39]. However, the length scales relevant for the mechanical properties of structural components (µm to mm-scale [40,41]) are not reached in metallic thin films. For example, the influence of grain size distribution and texture cannot be sufficiently analyzed [42] and a downstream step via the casting route is required, which reduces the time efficiency regarding the RAD. An advantage of RAD using AM-processes such 3D-EHLA is the manufacturability of bulk samples with a microstructure of comparable physical length scales (multiple grains, texture) as with a wide range of manufacturing methods (both conventional and AM). To exploit this advantage, particular attention must be paid to ensuring that the manufactured samples are free of defects. Otherwise, mechanical characteristics of the alloys such as tensile strength and elongation at break cannot be determined correctly. It is also possible to use the samples produced by 3D-EHLA only as a first step in the alloy development process and e.g. only measure the hardness instead of producing tensile specimen. The following chapter discusses whether the 3D-EHLA process is suitable for the RAD and which characteristics are necessary for the fabrication of bulk alloy libraries.

3.2 TOOLS AND PARAMETERS

Powder-gas jet

Small powder focus diameters enable an increased powder efficiency even with a high spatial resolution [43], which favors the economical production of fine structures such as tensile specimens for use in RAD. In addition, when using several different powders, care must be taken to ensure an even energy input per powder particle by the laser beam. A decrease of the powder focus leads to a more homogeneous heating [44]. Since the different elements required for the RAD already have different melting and boiling points, the process should not introduce any additional variables in this area. This is achieved by a small powder focus, as is the case with coaxial powder nozzles [43,44]. In order to adjust the powder mass flow $_{powder}$, the size of the annular gap can be varied in the range of 100-500 µm [45]. However, $_{powder}$ and thus the annular gap width should not be varied during a

process run to ensure process stability. Albeit, this only refers to the total powder mass flow. It must be noted that the volume flow increases due to density differences, when a less dense element is used at a fixed powder mass flow. It is therefore necessary to check, whether the volume flow should be selected as the measured variable to be kept constant in order to prevent blockages of the annular gap.

The alloy composition can be dynamically adjusted for the RAD by varying the individual powder mass flows of the different powder hoppers during a process cycle, as long as the total flow remains constant. The energy input into the powder particles and thus the melting behavior can be adjusted when considering the powder-gas jet via the particle velocity $v_{particle}$ as well as the powder mass flow $_{powder}$. When the conveying gas volume flow $\dot{V}_{CG}$ is increased, $v_{particle}$ increases, which leads to a shorter exposure time of the particles in the laser beam and thus to reduced heating. Likewise, an increase in $_{powder}$ leads to reduced heating of the particles in the beam path due to shielding effects [46]. In order to use the powder-gas jet for the RAD, both $v_{particle}$ and $_{powder}$ must be properly adjusted to ensure a complete melting of all alloying elements. If it is not possible to melt all elements homogeneously due to widely differing melting temperatures, either the alloy composition must be changed or the melt pool must be maintained for a longer period of time to enable all elements to be melted.

Laser radiation

In general, the laser radiation emitted in the 3D-EHLA process is used to melt the powder particles and create a melt pool on the substrates surface. It is particularly relevant for the RAD that the particle size has an influence on the melting behavior of the powder particles. The smaller the particle size, the faster the particles are melted [44]. If the laser power is increased too much and different elementary powders are used, heterogeneous evaporation can occur if the boiling point of some elements is exceeded. As a result, the final alloy composition can deviate from the theoretically calculated values [46]. In addition, an increased laser power can increase the size of the melt pool to such an extent, that the layer mixes heavily with the substrate due to high dilution (> 5%). This can also lead to a different alloy composition in the deposited layer. To counteract this phenomenon in case of graded samples, several layers of the same composition should be applied before the individual powder feed rates are adjusted and a new alloy is deposited. It is always necessary to consider the interactions of all parameters to avoid excessive dilution (> 5%), while also ensuring a sufficient melt pool size for the homogenization of the deposited layer. If the process speed is increased while assuming an approximately speed-insensitive powder-gas jet, the powder particles have the same exposure time to the laser radiation, but not the substrates surface. It is exposed to the laser radiation for a shorter duration, which leads to a smaller melt pool and a smaller heat-affected zone (HAZ) [44]. In order to facilitate the additive build-up of samples for alloy development, it must be ensured that the size of the melt pool is sufficient for a stable, melt-metallurgical bond at all times.

Powder properties

In addition to the chemical composition, a characterizing property of metallic powders is the individual particle morphology, which depends on the manufacturing method. Gas atomized powders have a spherical shape, while water atomized powders are more irregularly shaped [47]. Since powder flowability is increased for spherical powders, RAD should be performed with gas-atomized powders [47]. Although larger powder particles should be used to improve the ongoing flow behavior [47], a homogeneous mixing of the different powders becomes more difficult with increasing particle

size. Therefore, a trade-off between the flow behavior and the degree of mixing is necessary. It should also be noted that the annular gap of the coaxial powder nozzle used must not be clogged under any circumstances. If the particle size increases, a larger annular gap is required [44]. In addition to all these properties, the particle size distribution (PSD) also influences the process, since differences in particle size affect melting times of the particles in the beam path. In summary, gas-atomized particles with a narrow particle size distribution should be used for the RAD. Additionally, care must be taken when handling elements of different densities to ensure that the volume flow does not lead to a blockage of the annular gap. If possible, the various powder hoppers should be loaded with powders that are manufactured and dimensioned similarly. This helps to establish a uniform powder transport and thus a composition close to that of the desired alloy. Only in case of big differences in melting points or absorption coefficients, powders with different PSDs should be used to prevent heterogeneous evaporation and hence ensure a fitting alloy composition.

Process Speed

The relative movement between the process head and the substrates surface is referred to as the process speed. A high volume-build-up rate combined with a high spatial resolution can only be achieved by increasing the process speed [9]. A high spatial resolution is necessary if an intricate geometry is needed for a characterization process. Depending on the desired sample geometry, however, a lower spatial resolution can also be sufficient to generate samples for screening using RAD. If the production takes place with a lower spatial resolution, the volume build-up rate can be increased and thus the sample production can be accelerated. The relationship between volume build-up rate and the resulting microstructure has not been investigated yet. Furthermore, a change in process speed can lead to phase transitions due to the positive correlation between cooling rate and process speed [48]. DADA et al. have investigated HEAs such as AlCoCrFeNiCu by XRD and found that an increase in process speed leads to more prominent BCC peaks in the diffractogram [48]. They attributed this phase transition to the higher cooling rates at higher process speeds. If an alloy library with varying cooling rates is manufactured, the phase transitions of the individual alloy must be considered during the characterization.

Laser-beam particle interaction zone

In order to enable the manufacturing of three-dimensional samples using the 3D-EHLA process, the tools powder-gas jet and laser radiation as well as the parameters powder properties and process speed must interact with each other. If the aspect ratio (track width/height) is insufficient, pores can form between the layers [44], which leads to the formation of a defective microstructure and changed mechanical properties such as reduced tensile strength. Furthermore, it is a process-inherent requirement that both the powder particles and the substrate surface are melted [44]. While the powder particles are almost completely melted during the flight phase, the melt pool on the substrates surface should be kept as small as possible to ensure small dilution (< 5%) and therefore a composition close to that of the desired alloy. Since the laser radiation enables melting, increasing the laser power leads to an increase in temperature for both the particles and the substrate. When the working distance is increased, the powder particles are exposed to the laser radiation for a longer time and are therefore heated more [44], while the substrates surface is reached by decreasing amounts of focused radiation and cools down. This can lead to heterogeneous evaporation and the formation of pores in the sample due to lack of fusion defects [49]. When the conveying gas volume flow is increased, the particle

speed increases and the exposure time of the powder particles in the laser radiation is reduced, which leads to less heating and lowers the risk of heterogeneous evaporation [44]. Contrarily, the substrate temperature increases with increasing conveying gas volume flow, since more laser radiation is transmitted through the powder-gas jet and reaches the substrate surface due to the increased particle speed. If the powder mass flow increases, the particle temperature decreases due to shadowing effect between the individual powder particles [44]. The substrate temperature also decreases with increased powder mass flow due to shadowing effects caused by the denser powder-gas jet [44]. It has been shown that the process parameters have different influences regarding the heating of the powder particles and the substrate surface and therefore the alloy formation. All parameters listed in this chapter as well as parameters described in previous chapters such as process speed and particle size must be weighed against each other when used for the RAD.

4. METHODOLOGY

In view of the focus of this work on AM, the methodology must enable the development of alloys specifically for AM processes as well as for conventional melt-based processes such as casting. By changing the process parameters with 3D-EHLA, cooling rates from 10^2-10^7 K/s can be achieved [9]. Therefore, the emulation of the cooling conditions of both conventional processes such as direct chill casting (10^2 K/s [8]) as well as other AM-processes like LPBF (10^5-10^6 K/s [50]) is possible. This allows for an alloy development tailored to the final manufacturing method. Furthermore, the efficiency and knowledge gain must be increased by means of computer-aided analysis methods which are pooled in the ICME approach, such as CALPHAD or microstructure simulation [51]. There must be an integrated approach, in which the entire process chain of alloy development is covered by the methodology, starting from initial computer calculations to sample production and subsequent characterization. A methodology like this has been published and successfully implemented by DIPPO et al., where an alloy library of 16 samples was fabricated by LMD in a circular shape to enable a highly automatized characterization [3]. The planning of experiments is particularly difficult when considering multiple input factors. In addition to the conventional approach of an isolated change of one parameter after the other, statistical design of experiments (DoE), in which several variables are varied simultaneously, can be used. This reduces the number of necessary tests, while the influences of the individual parameters are determined using statistical methods. Especially when the manufacturing of many different samples in a short time is desired (e.g. for a DoE analysis), AM-processes like 3D-EHLA are superior compared to the traditional casting route.

In the processing of metallic materials using RAD, alloy libraries with a composition gradient or a microstructure gradient can be manufactured. A composition gradient is examined either discretely, i.e. by incrementally varying the composition in individual samples, or continuously by producing a sample with a composition that varies across the cross-section. A microstructure gradient is achieved by continuous variations of the thermal influences on the sample. The methodology used must be able to produce as many of these alloy libraries as possible. This is achieved by the usage of a process that allows for a wide variation in terms of both composition and the formation of different microstructures. In addition, the alloy composition should be able to be changed quickly and preferably during the ongoing process (in situ). With 3D-EHLA, the composition is easily adjustable by using differently loaded powder hoppers and the process conditions and thus the microstructure are changeable by varying parameters like the laser power or the process speed. Since all the requirements are met in the 3D-EHLA process, it is suitable for agile alloy development. However,

it is important to note that the characterization and not the sample production is the bottleneck for alloy development by means of the 3D-EHLA process [3].

5. EXPERIMENTAL PROCEDURE

The properties of alloys are determined not only by the composition, which can be variably adjusted in the 3D-EHLA process using multiple powder hoppers, but also by the microstructure. This is particularly true when considering the mechanical properties, which play a central role in construction and mechanical engineering. Therefore, the influence of the process parameters on the microstructure formation needs to be considered when applying 3D-EHLA for RAD. As of today, however, the correlations between process parameters and resulting microstructure are mostly unknown. First investigations on 316L EHLA single tracks show a significant decrease of the cell size with increasing process speed and increasing laser spot diameter [52]. Other parameters (laser power, powder focus position, shielding and conveying gas flow, powder mass flow) do not show a significant influence on the cell size [52].

The parameters to be varied in this work are the laser power P_L and the process speed v_P, since both parameters have an influence on the particle or substrate temperature in bulk deposition [44]. In addition, the powder mass flow $\dot{m}_P$ is varied to investigate its influence on the formation of the microstructure and to explore the possibility of accelerating sample production by increasing the volume build-up rate. The relative density as well as the average cell size are selected as assessment parameters. For this purpose, a full factorial DoE analysis with three levels and two variable parameters, laser power and process speed, is performed. In addition, the powder mass flow is varied at an otherwise fixed parameter combination.

All tests are carried out with a laser beam diameter d_L of 1,2 mm, a conveying gas volume flow $\dot{V}_{CG}$ of 10 l/min and a shielding gas volume flow $\dot{V}_{SG}$ of 6 l/min. All samples are manufactured with the same scan strategy (circular reversal, 14 tracks, 40 layers). The standard powder mass flow used is 33 g/min. The sample name contains the parameters used, e.g. sample V35P2240 is manufactured at a process speed of 35 m/min and a laser power of 2240 W.

Sample production using the 3D-EHLA process is carried out on a pE3D system by ponticon GmbH. 316L (1.4404) is used as a filler material. The MetcoAdd 316L-A powder used has a grain fraction of -45+15 µm, and a Metcotwin 150 is used as the powder feeder. Furthermore, an ILT COAX 40 powder nozzle and a TruDisk 4002 laser are used.

Construction steel substrate plates are used. The samples are cut parallelly to the build-up direction and perpendicularly to the process direction. Relative density is determined by light microscopy using a Keyence VHX-6000. The areas of high porosity within each sample are chosen, which is why the relative density values measured are to be understood as the lower limit. The polished samples are then etched using V2A etchant for 2,5 min. Finally, a cell size determination is carried out on the etched samples, with the average cell size determined over 30 cells. Preferably, round cells are measured, while in the case of stretched cells, the smallest dimension is measured. The cell size is measured in the middle of the upper half of the sample for all samples to level out the cooling influence of the substrate.

6. RESULTS

After the production of sample V65P4000, process build-up was found on the powder nozzle, which is attributed to the maximum laser power of 4000 W. In order not to damage the nozzle, the samples V35P4000 and V50P4000 are not manufactured.

The relative densities of the individual samples are listed in Table 1.

Table 1: Relative densities of the samples

		Laser power		
		2240 W	**3200 W**	**4000 W**
Process speed	**35 m/min**	99,5%	99,9%	-
	50 m/min	99,8%	99,8%	-
	65 m/min	98,7%	99,7%	99,6%
Process speed and powder mass flow	**50 m/min & 23,1 g/min**	-	99,3%	-
	50 m/min & 42,9 g/min	-	99,6%	-

Except for sample V65P2240 and V50P3200M23,1, all samples have a relative density of ≥ 99,5% in the area measured.

In the following figures, microsections of individual samples are shown.

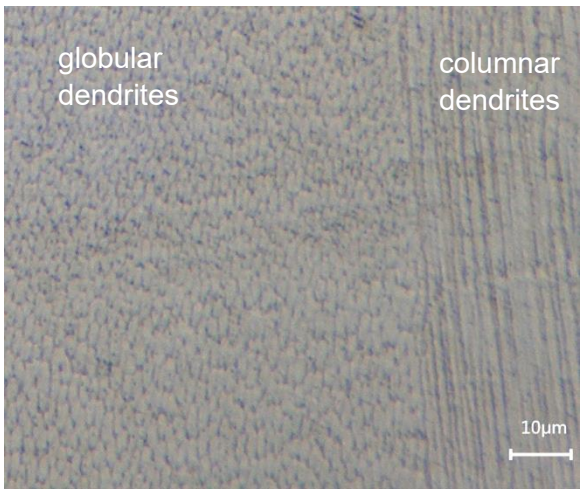

Fig. 2: sample V50P3200, etched, 2000x magnification

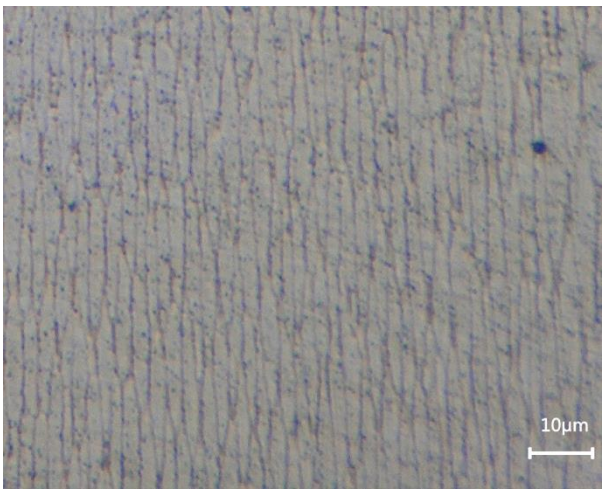

Fig. 3: sample V35P3200, etched, 2000x magnification

The cells of sample V35P3200 are visibly larger than the cells of sample V50P3200.

The average cell sizes determined from the microsections are used to determine the influence of the parameters laser power, process speed and powder mass flow on the cell size. The relationships are shown in the following diagrams.

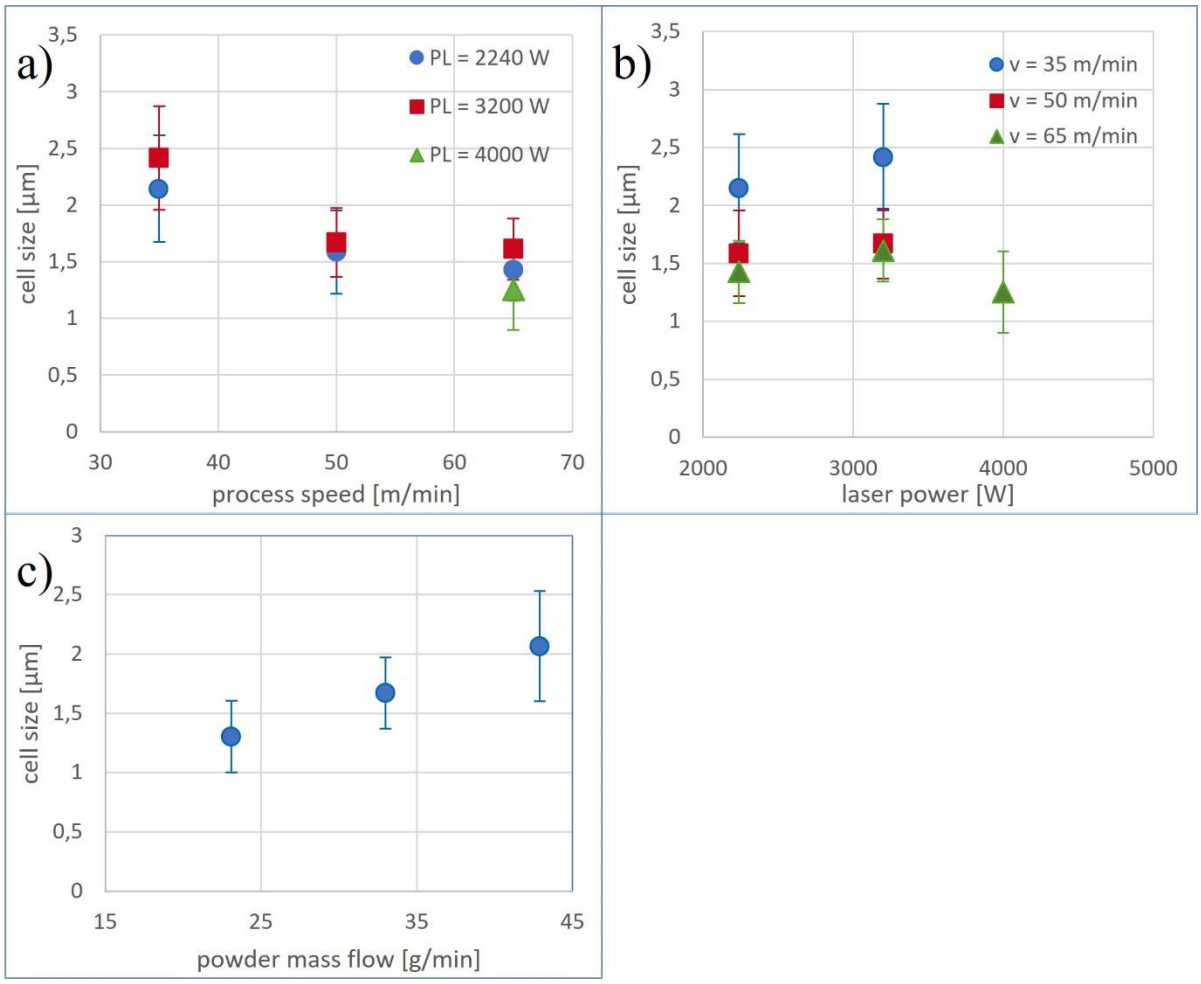

Fig. 4: Influence of a) process speed, b) laser power and c) powder mass flow on cell size

The process speed shows a negative correlation with the cell size, while the laser power and the powder mass flow show a positive correlation. The measured values of the sample V65P4000 deviate from these relationships. This is also the only sample that was produced with the maximum laser power of 4 kW and where process buildup was observed on the powder nozzle. The error bar in the measured cell sizes corresponds to the standard deviation of the 30 values measured.

7. DISCUSSION

The relative densities (Table 1) differ between the individual samples. A possible reason for a reduced relative density is an undersized melt pool, which can cause adhesion problems in the sample. The line energy density E_L is used as a suitable comparison parameter for the melt pool size.

$$E_L = \frac{P_L}{v_P} \tag{1}$$

The greater the line energy density, the larger the melt pool. For the samples examined (see Table 1), a positive correlation between relative density and line energy density is present. Sample V65P2240, which has the lowest relative density, also has the lowest line energy density at 2068 J/m. Sample V35P3200 has both the highest relative density and the highest line energy density at 5486 J/m. This positive correlation between line energy density and relative density is consistent with the findings of SUN et al. for LPBF [53] and GONG et al. for LMD [54]. However, it should be noted that above a

threshold value, the relative density decreases with increasing the line energy density due to the formation of gas pores [49]. Since the line energy density shows a positive correlation with the relative density in the samples examined, it is assumed that gas pores only form above 5486 J/m in the 3D-EHLA process. The reduced relative densities at low line energy densities can be attributed to adhesion errors [49].

The microstructure depicted in Fig. 2 features a globular dendritic microstructure on the left side of the image, while the microstructure on the right side is mainly columnar dendritic. However, it is also possible that the same solidification morphology occurs in both areas, while the visual difference between the structures is due to the cutting plane. If a columnar dendrite is cut perpendicular to the direction of growth, the structure appears globulitic. In general, there is mainly a columnar dendritic growth present in LMD-like processes [55]. A mainly columnar dendritic microstructure also is the norm with LPBF, where cooling rates similar to 3D-EHLA are present [56,57]. In such AM processes, the columnar dendrites are created by epitaxial growth on the grains/cells of the melted substrate [58]. Therefore, the texture of the adjacent layer has an influence on the growth of the deposited layer. The morphology of the layers is generally influenced by the quotient of temperature gradient G [K/m] and solidification rate R [m/s] [59]. The microstructure figure of the other sample (Fig. 3) mainly shows a columnar dendritic structure.

Increasing the process speed leads to a reduced cell size in the samples examined (Fig. 4a). In general, the cell size decreases when the cooling rate [K/s] increases due to increased nucleation [60]. This means that increases with an increase of the process speed. The cooling rate can be expressed as the product of G and R at the solidification front. The solidification rate increases with increasing process speed and can at most be equal to it. The temperature gradient also increases with increased process speed due to the reduced melt pool size [61–63]. Since both G and R increase with increasing process speed, increases with increasing process speed and the cell size is reduced.

Increasing the laser power leads to an increase in cell size in the samples examined (Fig. 4b). Therefore, must decrease by increasing the laser power. In previous studies done by BOLD et al. however, the influence of the laser power was found to not be significant in single tracks of 316L manufactured by EHLA [52]. This was attributed to the prevalent cooling influence of the substrate and the comparatively low energy input of manufacturing single tracks. Since the size of the melt pool increases with increased laser power, G decreases [62,64,65]. R also decreases with increasing laser power [62,66], since the increased heat input reduces the ratio of melt pool surface to volume and thus the heat transfer. Thus, both G and R are reduced with increasing laser power, which leads to a reduced and an increased cell size [67,68].

An increase in the powder mass flow leads to an increase in cell size in the samples examined (Fig. 4c). This requires a reduced when increasing the powder mass flow. An increase in the powder mass flow increases the cross-sectional area of the melt pool [69]. In addition, the maximum temperature at the melt pool surface is reduced [64]. Therefore, increasing the powder mass flow leads to a reduction in G. In the literature, an increased powder mass flow also leads to a reduced [70,71], while there is no clear correlation between the powder mass flow and R [62].

8. SUMMARY & OUTLOOK

Within this work, the scientific research status in the areas of AM and RAD is first determined. Based on this, the need for accelerated alloy development is illustrated by the largely unexplored phase space of new materials such as HEAs and the lack of processability of these using conventional manufacturing processes. After characterizing the challenges posed in the EHLA process, the novel 3D-EHLA process is established, which enables additive manufacturing using EHLA technology. Subsequently, the available tools and parameters of the 3D-EHLA process are presented and their individual influence on the alloy development is worked out. Furthermore, the suitability of the 3D-EHLA process for the application of the RAD is assessed.

Advantages of the 3D-EHLA process include the adaptability of the alloy composition in situ by varying the powder mass flow and the variation of the cooling rate by adjusting process parameters. Challenges of the 3D-EHLA process are heterogeneous evaporation due to different melting points of the metal powders used and ensuring an adhesion to the substrate that is sufficient for a low-defect bond. Also, the correlation between process parameters and solidification conditions are still under investigation, which is why the influence of laser power, process speed and powder mass flow on the formation of the microstructure are experimentally determined. The process speed shows a negative correlation to the cell size, while the laser power and the powder mass flow show a positive correlation.

Accelerated alloy development and the materials developed as a result can contribute to overcoming technological hurdles caused by material influences. The implications presented in this work for the RAD using the 3D-EHLA process are by no means complete, but they do represent a basis for further investigations. The following topics, among others, come into question:

- Influence of other process parameters such as the conveying gas volume flow on the composition and microstructure
- Building of a public database in which alloy-specific specialist knowledge is bundled, thus accelerating alloy development worldwide
- Scaling the manufacturing process used for the RAD to produce fully functional components using the same process
- Possibilities of overcoming the limitations of the 3D-EHLA process (e.g. heterogeneous evaporation, adhesion errors)
- Evaluation of possible uses of machine learning-supported test planning and evaluation to further reduce the required number of samples

REFERENCES

[1] A. García-Sánchez, D. Siles, M.d.M. Vázquez-Méndez, Competitiveness and innovation: effects on prosperity, Anatolia 30 (2019) 200–213. https://doi.org/10.1080/13032917.2018.1519179.

[2] A. Jain, S.P. Ong, G. Hautier, W. Chen, W.D. Richards, S. Dacek, S. Cholia, D. Gunter, D. Skinner, G. Ceder, K.A. Persson, Commentary: The Materials Project: A materials genome approach to accelerating materials innovation, APL Materials 1 (2013) 11002. https://doi.org/10.1063/1.4812323.

[3] O.F. Dippo, K.R. Kaufmann, K.S. Vecchio, High-Throughput Rapid Experimental Alloy Development (HT-READ), 2021.

[4] H. Springer, D. Raabe, Rapid alloy prototyping: Compositional and thermo-mechanical high throughput bulk combinatorial design of structural materials based on the example of 30Mn–1.2C–xAl triplex steels, Acta Materialia 60 (2012) 4950–4959. https://doi.org/10.1016/j.actamat.2012.05.017.

[5] R. Lachmayer, K. Rettschlag, S. Kaierle (Eds.), Konstruktion für die Additive Fertigung 2019, Springer Vieweg, Berlin, Heidelberg, 2020.
[6] C. Haase, F. Tang, M.B. Wilms, A. Weisheit, B. Hallstedt, Combining thermodynamic modeling and 3D printing of elemental powder blends for high-throughput investigation of high-entropy alloys – Towards rapid alloy screening and design, Materials Science and Engineering: A 688 (2017) 180–189. https://doi.org/10.1016/j.msea.2017.01.099.
[7] P.A. Hooper, Melt pool temperature and cooling rates in laser powder bed fusion, Additive Manufacturing 22 (2018) 548–559. https://doi.org/10.1016/j.addma.2018.05.032.
[8] S.W. Xu, K. Oh-ishi, S. Kamado, H. Takahashi, T. Homma, Effects of different cooling rates during two casting processes on the microstructures and mechanical properties of extruded Mg–Al–Ca–Mn alloy, Materials Science and Engineering: A 542 (2012) 71–78. https://doi.org/10.1016/j.msea.2012.02.034.
[9] T. Stittgen, Von der Beschichtung bis zur agilen Materialentwicklung: Potenziale und Herausforderungen bei der Anwendung des 3D-EHLA-Verfahrens, 2021.
[10] ponticon, Agile Legierungsentwicklung - ponticon, 2021. https://ponticon.de/anwendungen/anwendungen-2-3 (accessed 5 November 2021).
[11] D.P. Tabor, L.M. Roch, S.K. Saikin, C. Kreisbeck, D. Sheberla, J.H. Montoya, S. Dwaraknath, M. Aykol, C. Ortiz, H. Tribukait, C. Amador-Bedolla, C.J. Brabec, B. Maruyama, K.A. Persson, A. Aspuru-Guzik, Accelerating the discovery of materials for clean energy in the era of smart automation, Nat Rev Mater 3 (2018) 5–20. https://doi.org/10.1038/s41578-018-0005-z.
[12] G.M. Pharr, E.P. George, M.L. Santella, Development of Combinatorial Methods for Alloy Design and Optimization, 2005.
[13] A. Sviridov, I. Sizova, M. Bambach, Fast Development of New Alloys for Metal Forming Using Additive Manufacturing, in: G. Daehn, J. Cao, B. Kinsey, E. Tekkaya, A. Vivek, Y. Yoshida (Eds.), Forming the Future: Proceedings of the 13th International Conference on the Technology of Plasticity, firstst ed. twentiethtwenty-first, Springer International Publishing; Imprint Springer, Cham, 2021, pp. 1893–1902.
[14] B. Cantor, I. Chang, P. Knight, A. Vincent, Microstructural development in equiatomic multicomponent alloys, Materials Science and Engineering: A 375-377 (2004) 213–218. https://doi.org/10.1016/j.msea.2003.10.257.
[15] Y.F. Ye, Q. Wang, J. Lu, C.T. Liu, Y. Yang, High-entropy alloy: challenges and prospects, Materials Today 19 (2016) 349–362. https://doi.org/10.1016/j.mattod.2015.11.026.
[16] J.-W. Yeh, S.-K. Chen, S.-J. Lin, J.-Y. Gan, T.-S. Chin, T.-T. Shun, C.-H. Tsau, S.-Y. Chang, Nanostructured High-Entropy Alloys with Multiple Principal Elements: Novel Alloy Design Concepts and Outcomes, Adv. Eng. Mater. 6 (2004) 299–303. https://doi.org/10.1002/adem.200300567.
[17] C. Moreau, The State of 3D Printing 2020 edition - by Sculpteo (2020).
[18] B.W. Martin, Development of a novel, bicombinatorial approach to alloy development, and application to rapid screening of creep resistant titanium alloys, 2017.
[19] S. Ewald, F. Kies, S. Hermsen, M. Voshage, C. Haase, J.H. Schleifenbaum, Rapid Alloy Development of Extremely High-Alloyed Metals Using Powder Blends in Laser Powder Bed Fusion, Materials (Basel) 12 (2019). https://doi.org/10.3390/ma12101706.
[20] W.M. Steen, R.M. Vilar, K.G. Watkins, M.G.S. Ferreira, P. Carvalho, C.L. Sexton, M. Pontinha, M. McMahon, Alloy system analysis by laser cladding, in: International Congress on Applications of Lasers & Electro-Optics, Orlando, Florida, USA, Laser Institute of America, 1993, pp. 278–287.
[21] T. Schopphoven, A. Gasser, G. Backes, EHLA: Extreme High-Speed Laser Material Deposition, LTJ 14 (2017) 26–29. https://doi.org/10.1002/latj.201700020.
[22] T. Schopphoven, J.H. Schleifenbaum, S. Tharmakulasingam, O. Schulte, Setting Sights on a 3D Process, PhotonicsViews 16 (2019) 64–68. https://doi.org/10.1002/phvs.201900041.
[23] G. Marchese, X. Garmendia Colera, F. Calignano, M. Lorusso, S. Biamino, P. Minetola, D. Manfredi, Characterization and Comparison of Inconel 625 Processed by Selective Laser Melting and Laser Metal Deposition, Adv. Eng. Mater. 19 (2017) 1600635. https://doi.org/10.1002/adem.201600635.
[24] J. Yu, M. Rombouts, G. Maes, F. Motmans, Material Properties of Ti6Al4V Parts Produced by Laser Metal Deposition, Physics Procedia 39 (2012) 416–424. https://doi.org/10.1016/j.phpro.2012.10.056.
[25] H. Gurk, M. Brucki, R. Mayer, Frequenz- und Modalanalyse laserbeschichteter Bremsscheiben, in: R. Mayer (Ed.), Berichte aus dem Fahrzeugsystemdesign 2021, firstst ed. twentiethtwenty-first, Springer Fachmedien Wiesbaden; Imprint Springer Vieweg, Wiesbaden, 2021, pp. 33–49.
[26] Hornet, EHLA | Hornet Laser Cladding, 2022. https://www.hornetlasercladding.com/ehla (accessed 9 January 2022).
[27] J. Schaible, L. Sayk, T. Schopphoven, J.H. Schleifenbaum, C. Häfner, Development of a high-speed laser material deposition process for additive manufacturing, Journal of Laser Applications 33 (2021) 12021. https://doi.org/10.2351/7.0000320.
[28] R. Rauter, Laserauftragschweißen von Wolframkarbidschichten in Nickelbasismatrizen zur Herstellung verschleißfester Beschichtungen von Warmformwerkzeugen: Masterarbeit (2016).
[29] R. Vollmer, Optimierung mittels Laserauftragschweißen hergestellter Beschichtungen für die Blechumformung: Dissertation (2016).
[30] H.D. Sonderoptiken, Harald Dickler Sonderoptiken, 2021. http://hd-sonderoptiken.de/de/ (accessed 28 November 2021).
[31] A. Holzer, S. Koß, S. Ziegler, J.H. Schleifenbaum, K. Schmitz, Extreme High-Speed Laser Material Deposition (EHLA) as High-Potential Coating Method for Tribological Contacts in Hydraulic Applications, in: U. Reisgen, D. Drummer, H. Marschall (Eds.), Enhanced Material, Parts Optimization and Process Intensification: Proceedings of the First International Joint Conference on Enhanced Material and Part Optimization and Process Intensification, EMPOrIA 2020, May 19-20, 2020,

Aachen, Germany, firstst ed. twentiethtwenty-first, Springer International Publishing; Imprint Springer, Cham, 2021, pp. 153–167.
[32] S.-K. Rittinghaus, J. Zielinski, Influence of Process Conditions on the Local Solidification and Microstructure During Laser Metal Deposition of an Intermetallic TiAl Alloy (GE4822), Metall Mater Trans A 52 (2021) 1106–1116. https://doi.org/10.1007/s11661-021-06139-2.
[33] H. Dickler, S. Tharmakulasingam, Powder on Demand, LTJ 14 (2017) 15–17. https://doi.org/10.1002/latj.201700028.
[34] J. Mangos, N. Birbilis, Aluminium Alloy Design and Discovery using Machine Learning, 2021.
[35] B.L. Boyce, M.D. Uchic, Progress toward autonomous experimental systems for alloy development, MRS Bull. 44 (2019) 273–280. https://doi.org/10.1557/mrs.2019.75.
[36] N.K. Katiyar, G. Goel, S. Goel, Emergence of machine learning in the development of high entropy alloy and their prospects in advanced engineering applications, emergent mater. (2021). https://doi.org/10.1007/s42247-021-00249-8.
[37] A.I. Mardare, A. Savan, A. Ludwig, A.D. Wieck, A.W. Hassel, High-throughput synthesis and characterization of anodic oxides on Nb–Ti alloys, Electrochimica Acta 54 (2009) 5973–5980. https://doi.org/10.1016/j.electacta.2009.02.104.
[38] A. Matthews, Titanium Nitride PVD Coating Technology, Surface Engineering 1 (1985) 93–104. https://doi.org/10.1179/sur.1985.1.2.93.
[39] J. Neidhardt, S. Mráz, J.M. Schneider, E. Strub, W. Bohne, B. Liedke, W. Möller, C. Mitterer, Experiment and simulation of the compositional evolution of Ti–B thin films deposited by sputtering of a compound target, Journal of Applied Physics 104 (2008) 63304. https://doi.org/10.1063/1.2978211.
[40] M. Bennoura, A. Aboutajeddine, Overall challenges in incorporating micro-mechanical models into materials design process, J. Phys.: Conf. Ser. 758 (2016) 12022. https://doi.org/10.1088/1742-6596/758/1/012022.
[41] G. Bolzon, B. Rivolta, Mechanical characterization of metals by small sampling size, Procedia Structural Integrity 21 (2019) 185–189. https://doi.org/10.1016/j.prostr.2019.12.100.
[42] H. Knoll, S. Ocylok, A. Weisheit, H. Springer, E. Jägle, D. Raabe, Combinatorial Alloy Design by Laser Additive Manufacturing, steel research int. 88 (2017) 1600416. https://doi.org/10.1002/srin.201600416.
[43] S. Jung, G. Backes, Koaxiale Pulverdüsen: Fraunhofer ILT (2014).
[44] T. Schopphoven, Experimentelle und modelltheoretische Untersuchungen zum Extremen Hochgeschwindigkeits-Laserauftragschweißen. Dissertation, Univ., 2019.
[45] S. Asche, EHLA: Mit extremer Hochgeschwindigkeit zum Bauteil: Podcast, Guest: Schleifenbaum, Johannes Henrich. from 33:45, 2020. https://www.ingenieur.de/technik/fachbereiche/medien/podcasts/druckwelle-3d-druck/ (accessed 4 December 2021).
[46] S. Koß, S. Ewald, M.-N. Bold, J.H. Koch, M. Voshage, S. Ziegler, J.H. Schleifenbaum, Comparison of the EHLA and LPBF Process in Context of New Alloy Design Methods for LPBF, AMR 1161 (2021) 13–25. https://doi.org/10.4028/www.scientific.net/AMR.1161.13.
[47] P. Kiani, U. Scipioni Bertoli, A.D. Dupuy, K. Ma, J.M. Schoenung, A Statistical Analysis of Powder Flowability in Metal Additive Manufacturing, Adv. Eng. Mater. 22 (2020) 2000022. https://doi.org/10.1002/adem.202000022.
[48] M. Dada, P. Popoola, N. Mathe, S. Pityana, S. Adeosun, O. Aramide, T. Lengopeng, Process optimization of high entropy alloys by laser additive manufacturing, Engineering Reports 2 (2020). https://doi.org/10.1002/eng2.12252.
[49] P. Ferro, R. Meneghello, G. Savio, F. Berto, A modified volumetric energy density–based approach for porosity assessment in additive manufacturing process design, Int J Adv Manuf Technol 110 (2020) 1911–1921. https://doi.org/10.1007/s00170-020-05949-9.
[50] H. Eskandari Sabzi, P.E. Rivera-Díaz-del-Castillo, Composition and process parameter dependence of yield strength in laser powder bed fusion alloys, Materials & Design 195 (2020) 109024. https://doi.org/10.1016/j.matdes.2020.109024.
[51] A.A. Luo, Material design and development: From classical thermodynamics to CALPHAD and ICME approaches, Calphad 50 (2015) 6–22. https://doi.org/10.1016/j.calphad.2015.04.002.
[52] M.-N. Bold, Investigation of Cooling Rate and Microstructure with the Aim of Alloy Development using Extreme High Speed Laser Material Deposition (EHLA) exemplified by 316L, 2021.
[53] K. Sun, W. Peng, L. Yang, L. Fang, Effect of SLM Processing Parameters on Microstructures and Mechanical Properties of Al0.5CoCrFeNi High Entropy Alloys, Metals 10 (2020) 292. https://doi.org/10.3390/met10020292.
[54] Y. Gong, Y. Yang, S. Qu, P. Li, C. Liang, H. Zhang, Laser energy density dependence of performance in additive/subtractive hybrid manufacturing of 316L stainless steel, Int J Adv Manuf Technol 105 (2019) 1585–1596. https://doi.org/10.1007/s00170-019-04372-z.
[55] S. Paul, J. Liu, S.T. Strayer, Y. Zhao, S. Sridar, M.A. Klecka, W. Xiong, A.C. To, A Discrete Dendrite Dynamics Model for Epitaxial Columnar Grain Growth in Metal Additive Manufacturing with Application to Inconel, Additive Manufacturing 36 (2020) 101611. https://doi.org/10.1016/j.addma.2020.101611.
[56] P. Mohammadpour, A.B. Phillion, Solidification microstructure selection maps for laser powder bed fusion of multicomponent alloys, IOP Conf. Ser.: Mater. Sci. Eng. 861 (2020) 12005. https://doi.org/10.1088/1757-899X/861/1/012005.
[57] H. Qin, V. Fallah, Q. Dong, M. Brochu, M.R. Daymond, M. Gallerneault, Solidification pattern, microstructure and texture development in Laser Powder Bed Fusion (LPBF) of Al10SiMg alloy, Materials Characterization 145 (2018) 29–38. https://doi.org/10.1016/j.matchar.2018.08.025.
[58] A. Basak, S. Das, Epitaxy and Microstructure Evolution in Metal Additive Manufacturing, Annu. Rev. Mater. Res. 46 (2016) 125–149. https://doi.org/10.1146/annurev-matsci-070115-031728.
[59] J.C. Lippold, Welding metallurgy and weldability, John Wiley & Sons Inc, Hoboken, New Jersey, 2015.

[60] S.B. Kang, S. Wang, J. Cho (Eds.), Effect of Cooling Rate on Microstructure and Mechanical Properties in Al-Si Alloys: The 12th International Conference on Aluminium Alloys, September 5-9, 2010 PACIFICO YOKOHAMA, Yokohama, Japan proceedings, pp. 675-680, Japan Institute of Light Metals, Tokyo, 2010.
[61] C. Hagenlocher, F. Fetzer, D. Weller, R. Weber, T. Graf, Explicit analytical expressions for the influence of welding parameters on the grain structure of laser beam welds in aluminium alloys, Materials & Design 174 (2019) 107791. https://doi.org/10.1016/j.matdes.2019.107791.
[62] J. Shao, G. Yu, X. He, S. Li, R. Chen, Y. Zhao, Grain size evolution under different cooling rate in laser additive manufacturing of superalloy, Optics & Laser Technology 119 (2019) 105662. https://doi.org/10.1016/j.optlastec.2019.105662.
[63] A. Segerstark, Laser Metal Deposition using Alloy 718 Powder: Influence of Process Parameters on Material Characteristics, 2017.
[64] S.J. Wolff, Z. Gan, S. Lin, J.L. Bennett, W. Yan, G. Hyatt, K.F. Ehmann, G.J. Wagner, W.K. Liu, J. Cao, Experimentally validated predictions of thermal history and microhardness in laser-deposited Inconel 718 on carbon steel, Additive Manufacturing 27 (2019) 540–551. https://doi.org/10.1016/j.addma.2019.03.019.
[65] Z. Wang, T.A. Palmer, A.M. Beese, Effect of processing parameters on microstructure and tensile properties of austenitic stainless steel 304L made by directed energy deposition additive manufacturing, Acta Materialia 110 (2016) 226–235. https://doi.org/10.1016/j.actamat.2016.03.019.
[66] A. Chiocca, F. Soulié, F. Deschaux-Beaume, C. Bordreuil, In situ observations and measurements during solidification of CuNi weld pools, Science and Technology of Welding and Joining 21 (2016) 578–584. https://doi.org/10.1179/1362171815Y.0000000091.
[67] G.A. Ravi, C. Qiu, M.M. Attallah, Microstructural control in a Ti-based alloy by changing laser processing mode and power during direct laser deposition, Materials Letters 179 (2016) 104–108. https://doi.org/10.1016/j.matlet.2016.05.038.
[68] A.A. Adeyemi, E.T. Akinlabi, R.M. Mahamood, K.O. Sanusi, S. Pityana, M. Tlotleng, Influence of laser power on microstructure of laser metal deposited 17-4 ph stainless steel, IOP Conf. Ser.: Mater. Sci. Eng. 225 (2017) 12028. https://doi.org/10.1088/1757-899X/225/1/012028.
[69] K. Shah, A.J. Pinkerton, A. Salman, L. Li, Effects of Melt Pool Variables and Process Parameters in Laser Direct Metal Deposition of Aerospace Alloys, Materials and Manufacturing Processes 25 (2010) 1372–1380. https://doi.org/10.1080/10426914.2010.480999.
[70] J.L. Bennett, S.J. Wolff, G. Hyatt, K. Ehmann, J. Cao, Thermal effect on clad dimension for laser deposited Inconel 718, Journal of Manufacturing Processes 28 (2017) 550–557. https://doi.org/10.1016/j.jmapro.2017.04.024.
[71] M. Ali Bagheri, Microstructural behavior and multiscale structure-property relations for cyclic loading of metallic alloys procured from additive manufacturing (Laser Engineered Net Shaping – LENS), 2017.